SSRG International Journal of Mechanical Engineering
ISSN: 2348-8360/ https://doi.org/10.14445/23488360/IJME-V12I5P105

Volume 12 Issue 5, 41-49, May 2025
2025 Seventh Sense Research Group®

Original Article

Design and Development of Innovative Test Rig for Analyzing Real-World Vehicle Conditions in Performance Evaluation of Automotive Composite Brake Pads

Rahul Dilip Pharande[1], Balaji Nagorao Sontakke[2], Ganesh Haribhau Kawade[3]

[1, 2]*Department of Mechanical Engineering, Chhatrapati Shivaji Maharaj University, Panvel, Maharashtra, India.*
[3]*Department of Automobile Engineering, D Y Patil University, Pune, Ambi, Maharashtra, India.*

[1]*Corresponding Author : rahuldpharande@gmail.com*

Received: 08 March 2025 Revised: 07 April 2025 Accepted: 06 May 2025 Published: 31 May 2025

Abstract *- This research article concentrated on creating a new environmentally friendly material for automotive brake pad applications and designing and developing a brake pad test rig to assess the performance of composite brake pads under regulated braking conditions. The aim is to create a pollution-free brake pad that enhances performance and durability and reduces weight. The design functionality was tested using specialized equipment to evaluate the performance of three composite brake pads. A test bench is presented to improve comprehension and testing of brake pads in automotive applications. The study incorporates the cooling rate of each brake pad, which was determined, and each composite brake pad's effectiveness was assessed using stopping time and temperature rise. The findings demonstrate that brake pads' wear rates are acceptable and in line with industry standards. When considering the cooling rate, temperature rise, and stopping distance, the basalt brake pad is the most efficient. The jute brake pad is the least effective, followed by glass and basalt fiber brake pads. Basalt brake pads offer the highest working efficiency with 42.5% cooling efficiency, while glass and jute brake pads provide 35.72% and 28.21% efficiency, respectively. Selected composite materials are best in stopping time and heat resistance compared to the other materials.*

Keywords *- Composite brake Pad, Test Rig Design, Performance of Brake Pad.*

1. Introduction

Automobile vehicles are now a commonplace aspect of daily life, used for transportation on highways and other flexible surfaces. The braking system is crucial to the safe, efficient functioning and management of these vehicles since it needs to slow down the vehicle more quickly than the engine can accelerate [1]. The brake disc system and the brake drum system are the two varieties of braking systems. Cars can have disc brakes, drum brakes, or a mix of the two. A disc brake's caliper, rotor, and friction brake pads are its three primary parts. The braking system's friction brake material is a crucial component. The friction materials and brake pads are the most important components of the brake systems that affect braking performance and driving safety [2]. We chose three types of composite brake pads to achieve satisfactory performance compared to asbestos-based and ceramic-based brake pads to provide satisfactory performance while minimizing environmental impact. Brake pads should, therefore, have a constant coefficient of friction, low rate of wear, low noise level, anti-vibration properties, and an improved cooling rate, even in demanding driving conditions. Also, they should be comfortable, strong, and safe. When replacing brake pads, consumers have a variety of friction materials to choose from. However, it is essential that the replacement pads match or exceed the performance of the original linings [3]. In industries without established standards for brake pad quality and performance, consumers are at risk of purchasing substandard replacements. These inferior brake pads can compromise braking efficiency, potentially leading to unexpected brake system failures while in use.

In addition to the materials and hardware design of the vehicle, driver behaviour, vehicle usage, the brake system's level of adjustability, and the general driving environment all have a big impact on brake performance [4]. In addition to these factors, braking control systems may be impacted by engine braking and wheel system alignment [5-7]. There are four varieties of these test devices: Chase-type machines, pin-on-disc tribometers, inertial dynamometers (ECE R-90 standard test), and Friction Assessment and Screening Test (FAST) [8]. The three main parts of these friction machines are a system for detecting frictional torque, a force application mechanism, and a conformal contact mechanism. Some tests need deceleration, and others require a steady speed. Both temperature measurement deceleration and multiple-load applications are frequently used [9]. While many researchers use laboratory-type devices to measure the wear and friction properties of metal and natural powder automotive brake pads, some researchers use simpler friction devices made for specimen-type pads [10, 11]. This paper presents the design, development, and testing of an experimental laboratory brake pad using a designed test rig, which can be integrated with an existing petrol engine. The test rig was utilized to assess the performance and quality of automotive friction brake pads by simulating the braking system and conditions of the vehicle in which the brake pads will be installed. It has also been noted that despite the use of various material tests, such as compression tests and thermal conductivity measurements while creating friction brake materials and spices, the final qualification process requires extensive on-vehicle testing with full-sized components [12]. Several testing machines have been developed to enhance brake system safety, performance predictability and reliability [13]. This paper presents the design, construction, and testing of a composite brake pad (Jute fibre, glass fibre, and Basal fibre) on the developed test rig, which can be integrated with an existing engine. The test rig was utilized to evaluate the performance and quality of automotive friction brake pads by simulating the braking system and operating conditions of the vehicle in which the pads will be installed.

The present work contains three main objectives. The first step is to present the test rig design for the new composite material for brake pad temperature and wear tests in accordance with the SAE standard. The second objective is to test the new design with composite material parallel to how friction testing equipment is used to evaluate their performance. The third goal is to suggest an experimental approach for assessing and testing novel composite materials for brake pad applications. Finally, the test results are utilized to compare the wear rates and temperature efficacy of three chosen composite brake pads and confirm that the test equipment fully operates satisfactorily.

2. Material and Methods

2.1. Selected Composite Brake Pad

Traditionally, brake pads were composed of asbestos fibres surrounded in a polymeric environment along with other chemical additives. Due to the hazardous nature of asbestos, it's no longer permitted. As a result, asbestos-free brake pads are now being developed using preferred natural fibers that are cost-effective, readily available, and recyclable [14]. Natural fibers are generally classified as those derived from minerals, plants, vegetables, animals, or agricultural waste, which can be processed into non-woven textiles. The friction material specimens for this test were created using a standard Non-Asbestos Organic (NAO) formulation. For the selection of composite materials, it was essential to consider the engineering properties of the brake pads, with particular emphasis on their physical and mechanical characteristics. In accordance with the required standards for brake pad materials, we ensured the proper wear rate, temperature coefficient, and hardness of the material through different mechanical tests.

Brake pads made of glass, basalt, and jute fibers were examined in this study since the selection of fibers greatly impacts material handling and overall performance. Brake pad production involves a number of unit procedures, such as mixing, cooling, post-curing, hot and cold pressing, and finally, finishing. The blended material is placed in a mould to shape the brake pad. A pre-pressing step compacts the material into a semi-finished product, ensuring uniform density and alignment of fibers. The schematic of the composite friction brake pad is illustrated in Figure 1.

Finally, these three materials are practiced on a specially designed setup. The brake pad tests aim to compare the wear rates and efficacy of the three types of commercially available automobile brake pads and to show how well the test rig works.

Fig. 1 Sample of composite brake pad

3. Design and Development of Brake Pad Test Rig

When designing a brake pad test setup, it's essential to base the design on the specific vehicle's parameters to ensure accurate simulation of real-world conditions. A crucial aspect of this setup is replicating the vehicle's mass moment of inertia, particularly the inertia experienced at maximum velocity. The setup design includes the necessary calculations and specifications of the flywheel. Radial and tangential stresses in the flywheel, shaft diameter of the motor, and bearing selection with required gear design for necessary ratios. The design details of the required components are discussed in the below section.

3.1. Mass Moment Inertia of Flywheel

To calculate the required mass moment of inertia, the first step is to determine the weight transfer occurring on the front axle of the selected vehicle. This involves analyzing the dynamic load distribution during acceleration or braking, the magnitude of the weight transfer to the front axle measured utilizing Equation (1) that follows.

$$\Delta R = \frac{(\mu \times g \times h \times M)}{l} \quad (1)$$

This equation provides the weight transferred to the front axle during braking, a critical parameter for accurately replicating braking conditions and understanding the forces exerted on the vehicle’s components. Calculating the weight transfer makes it possible to evaluate how well the braking system works, particularly under maximum braking conditions [15]. The total weight acting on the front axle during braking is the sum of the static weight already supported by the front axle and the additional weight transferred due to braking forces. Once the total weight on the front axle is determined, the corresponding mass can be calculated by dividing the total weight by the acceleration due to gravity, as illustrated below.

$$w_f = R_{fs} + \Delta R \quad (2)$$

$$m_f = \frac{w_f}{g} \quad (3)$$

This approach enables the precise determination of the effective mass on the front axle, a critical factor for simulating real-world braking conditions and ensuring that the test setup accurately reflects the vehicle's behavior under maximum load conditions.

The coefficient of friction and the mass acting on the front axle are pivotal in generating the frictional force between the tire and the road surface. This frictional force is essential for effective braking. The frictional force is calculated as the product of the weight acting on the front axle and the coefficient of friction between the tire and the road surface. Once the frictional force is determined, it is subsequently used to generate the maximum braking torque in combination with the tire radius. The braking torque represents the rotational force necessary to decelerate or halt the vehicle, and it is calculated as follows.

$$F = w_f \times \mu \quad (4)$$

$$T_B = F \times R \quad (5)$$

By understanding the relationship between the frictional force and braking torque, it is possible to accurately simulate and evaluate the braking performance of the vehicle under various conditions. The frictional force generated through the tire-road interaction, in conjunction with the braking torque, dictates the vehicle's ability to decelerate effectively. This is crucial for assessing brake pad performance within the test setup.

Since the mass on the front axle represents the energy stored in motion, the kinetic energy vehicle is precisely proportional to that mass [16]. In a similar vein, kinetic energy is linked to the mass moment of inertia of rotating devices, such as the flywheel. This relationship enables the determination of the mass moment of inertia for the flywheel in the test apparatus. The KE of the vehicle is stated as per Equation (6).

$$KE = \frac{1}{2} m_f V^2 \quad (6)$$

For a rotating body, KE is associated with mass inertia ‘I’ and the angular velocity (ω) as follows [17].

$$KE = \frac{1}{2} I \omega^2 \quad (7)$$

By equating the KE of the vehicle with the KE of the flywheel, the required mass moment of inertia (I) for the flywheel can be calculated. This ensures that the flywheel accurately replicates the energy conditions of the vehicle during braking, thereby facilitating precise testing of the brake system under realistic load conditions. Once the mass moment inertia for a single wheel is determined, the flywheel can be selected based on this value, which takes into account mass and radius [18]. The following formula is used to get the flywheel's mass moment of inertia.

$$I = \frac{1}{2} m r^2 \quad (8)$$

3.2. Tangential and Radial Stress in Flywheel

As a flywheel operates at high rotational speeds, it experiences significant stress, which increases the potential for catastrophic failure, such as fracturing or disintegration. This risk is particularly pronounced in the presence of manufacturing defects or if the flywheel exceeds its design speed limits. Evaluating the tangential and radial stresses applied to the material during operation is crucial for maintaining the flywheel's structural integrity and safety [19]. The maximum tangential stress (σ_t) and radial stress (σ_r) can be determined using the following equation.

$$(\sigma_t)_{max} = (\sigma_r)_{max} = \frac{\rho v^2}{10^6} \left(\frac{\mu_p + 3}{8}\right) \quad (9)$$

By ensuring tangential and radial stresses remain within the material's safe limits, the flywheel can operate securely at high rotational speeds, thereby minimizing the risk of failure while preserving its performance. This approach is essential for preventing material failure and enhancing the operational longevity of the flywheel in high-speed applications.

3.3. Design of Shaft

In this design test rig, two distinct shafts must be used, each serving a specific function. One of these shafts was a motor shaft, and another was a flywheel shaft. The motor shaft is responsible for supporting the gear with torsional moment. The torsional shear stress (τ) acting on this shaft is computed using the subsequent formula.

$$\tau = \frac{M_t \times R_s}{J} \qquad (10)$$

This approach ensures that the motor shaft is appropriately sized to withstand the torsional forces generated under typical operational conditions, thereby facilitating effective power transmission to the gear while accounting for the dynamic behavior of the vehicle during testing [20].

The second shaft, i.e., the flywheel shaft, is designed to support a heavy flywheel. This shaft is subjected to both torsional and bending moments, and its design is based on the combined effect of these forces. The equivalent moment for the flywheel shaft, which incorporates both torsional and bending moments, can be calculated using the following equation:

$$\sqrt{(\mathrm{K}_b \times M_b)^2 + (\mathrm{K}_t \times \mathrm{M}_t)^2} \qquad (11)$$

This equation accounts for the combined effects of bending and torsional stresses on the flywheel shaft, ensuring that the shaft is designed to withstand both types of loading without failure.

3.4. Selection of Bearing

The selection of a suitable bearing is primarily determined by key factors such as the shaft diameter, which matches the bearing's inner diameter, along with the bearing's load capacity and the shaft's operating speed. In this process, it is essential to consider both the radial and axial loads bearing encounters and the operational speed to ensure optimal performance and durability. In this application, a self-aligning ball bearing is chosen due to its ability to automatically adjust the shaft's axis, compensating for any misalignment that may arise during operation. To ensure the test setup operates efficiently, the motor's power output must exceed the system's frictional power losses [21]. These losses primarily stem from friction in the bearings and the gear train components. Bearings experience the highest frictional losses as they directly bear the flywheel's load. In contrast, the gear train encounters relatively lower friction losses due to the line contact between the gear and pinion faces. As a result, the motor must initially provide higher torque to overcome frictional losses in both the bearings and the gear train. The power loss at each bearing can be determined by calculating the frictional force and the corresponding torque applied to the bearing. Therefore, the motor chosen for the test setup must be capable of providing a power output that surpasses the total power losses from all bearings and the gear train, ensuring it can sustain the required load to drive the system effectively.

3.5. Selection of Gear Train Configuration

The primary function of the gear train in the system is to increase the flywheel's rotational speed, which is essential for achieving the required mass moment of inertia in the test setup. The flywheel's rotational speed is a key factor in determining its moment of inertia. To achieve the necessary speed amplification, the gear train design must consider both the gear ratio and the motor specifications. The power transmitted through the gear system is determined by the torque and speed, which allows for the evaluation of the gear module [22]. The gear module is calculated using the following expression 12.

$$m_g = \left[\frac{60 \times 10^6}{\pi}\left\{\frac{(kW) \times C_S \times (fs)}{z_p \times n_p \times C_V \times \left(\frac{b}{m}\right) \times \left(\frac{S_{ut}}{3}\right) \times Y}\right\}\right]^{1/3} \qquad (12)$$

The calculation of the gear module is verified by incorporating an appropriate safety factor. Once the module is determined, the size of the gear train and the required surface hardness can be calculated, ensuring that the design meets performance requirements and effectively handles the expected operating loads and speeds.

4. Operation of Brake Pad Test Rig

4.1 Specification of Test Rig

In order to produce a realistic braking environment, a designed test rig was made to regulate the installed components based on real-time data sampling from the sensors, with the ability to collect data in real-time; when an operator creates a scenario, the system delivers the operational conditions. It implies that the structure gives truthful measurement testing with a configurable number of braking tests and variable temperatures. Table 1 shows the technical specifications of the developed test setup. To determine the performance of the composite friction brake pad test setup, a photographic view and schematic structure of components are displayed in Figures 2 and 3, respectively.

Table 1. Specification of Brake Pad Test Rig

Parameters	**Specifications**
Motor	3 HP, 700 rpm, AC
Shaft diameter	50 mm
Bearings	2210 ZKL Bearing
Flywheel Weight	70 kg
Gear Ratio	5 :1
Gear Module	7 mm
Gear BHN	160
Temperature Sensors	K-type thermocouple and RTD (PT100)

Fig. 2 Photographic view of Brake Pad Test Setup

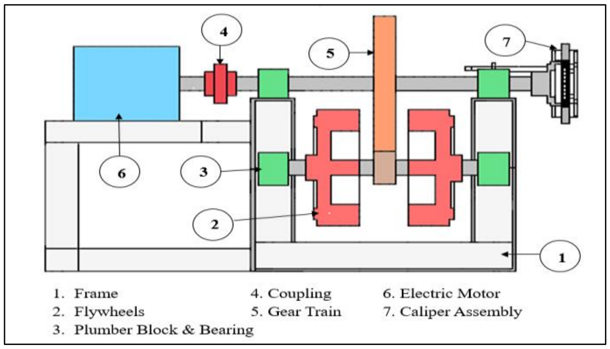

Fig. 3 Schematic Illustration of the Test Setup

4.2. Procedure of Brake Pad Test

Three types of composite brake pads were manufactured for testing purposes and labeled as Jute, Glass, and Basalt. The performance of each brake pad was assessed with the above-described brake pad test setup, maintaining a constant brake pedal force of 10 kg and brake pad contact pressure while varying the rotational motor shaft speed between 200 and 500 RPM.

In order to allow the rotating brake disc with the brake pad to gradually come to a complete stop, the brake pad test rig was assembled to rotate at a certain vehicle engine flywheel rotational speed. The engine flywheel is connected to the selected motor to activate the brake pad test rig assembly. This allows the rotating brake disc with the brake pad to gradually come to a rotation and complete stop. An adequate force is applied to the brake pad while the test and measurements taken, such as stopping time, temperature rise, and other pertinent characteristics, are recorded by applying forces to the pedal plate.

The stopping time is measured using a stopwatch, the temperature is recorded with a non-contact infrared temperature sensor, and the speed is simultaneously measured with a tachometer. Then, the previously tested brake pad is removed from the caliper and replaced with another composite brake pad for testing. After completion of the temperature rise and deceleration test, the electric motor is immediately restarted, and increased the motor shaft speed to 500 rpm.

Then, the motor is switched off, allowing the brake disc to rotate freely. Corresponding to this temperature, the rotational speed (rpm) of the brake pad and disc are recorded at one-minute intervals until the brake disc comes to a complete stop without applying braking forces. The collected data is then used to generate graphs of rotational speed versus time and temperature versus time. This approach facilitates evaluating the brake pad's cooling characteristics under dynamic conditions.

Using all required instruments, measurements were taken to evaluate the performance attributes of three different kinds of brake pads. Every test is conducted three times on a brake pad at a specific speed, and the final test result is determined by averaging the three results [23]. The average stopping time and temperature rise in different test conditions were measured and recorded. The recorded results of the three tested composite brake pads are mentioned in Table 2 and Table 3.

Table 2. Result of composite brake pad

Description	Speed (rpm)	Temperature		Time to Stop (Sec)
		Initial	Final	
Jute Fiber	200	32	52	30
	300	32	65	32
	400	30	72	36
	500	30	81	45
Glass Fiber	200	30	50	24
	300	32	57	27
	400	30	63	31
	500	32	70	35
Basalt Fiber	200	31	47	20
	300	32	52	22
	400	30	57	25
	500	31	63	31

Table 3. Cooling effect test result of composite brake pad

Time (min)	Jute Fiber		Glass Fiber		Basalt Fiber	
	Speed (rpm)	Temp (^{0}C)	Speed (rpm)	Temp (^{0}C)	Speed (rpm)	Temp (^{0}C)
0	500	81	500	70	500	63
1	412	77.6	420	66.4	415	59
2	335	74.4	340	61	338	54.7
3	260	71.8	264	57.5	258	48.4
4	205	68.2	198	53	210	44
5	150	64	145	49.6	160	41.3
6	110	62.1	103	47	109	39
7	75	59.8	80	46	78	37.3
8	35	58.5	30	45	40	36

5. Result and Discussions

The effectiveness of the brake pads was influenced by their ability to balance temperature control, pedal feel, deceleration, and stopping distance. The results show that the most effective brake pads delivered consistent performance across all evaluated criteria, although each type of brake pad had its own specific advantages.

5.1. Deceleration Performance of Brake Pad

Braking effectiveness is measured with deceleration, the degree to which a vehicle's brake system can effectively slow down or stop it. Braking effectiveness improves with higher deceleration rates [24]. Brake pads that generated more friction with the same applied force resulted in faster deceleration. This demonstrates how much the material and design of the brake pad affect the vehicle's stopping time. Figure 4 presents a plot of the average stopping time for the three types of composite brake pads under varying speed conditions, with a constant pedal force of 98.1 N and a contact pressure of 0.82 MPa.

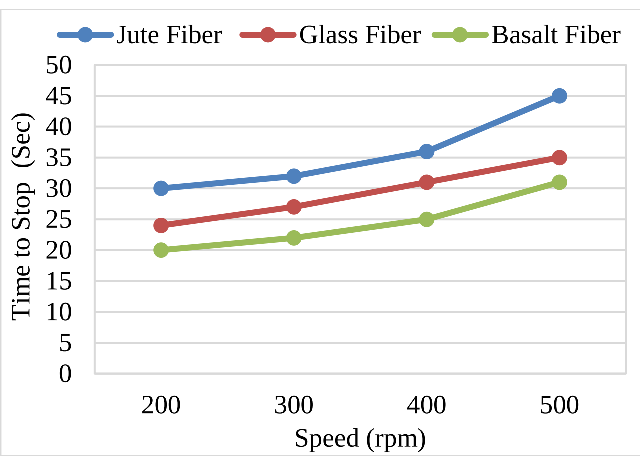

Fig. 4 Speed vs. Stopping Time of Brake Pad

From the graph, it is clear that at any given speed of the brake pad, the Jute fibre brake pad takes longer to stop than other brake pads due to lower friction and heat resistance. At the same time, the brake pad basalt has the shortest stopping time, while the glass fibre brake pad has a moderate stopping time between the jute basalt fibre brake pad. For all the brake pads, under the application of a constant force on the brake pedal, the stopping time increases as the speed increases.

The Basalt brake pad has the shortest stopping time. This is because brake pads made from basalt typically offer better coefficient of friction and thermal stability, leading to faster braking and more efficient heat dissipation than the other two types of composite brake pads [25].

5.2. Temperature Rise Test of Composite Brake Pad

The temperature rise test assesses how various brake pad compositions respond to heat when braking. Too much heat can cause brake fade, decreased performance, and increased wear, which are very important for the satisfactory characteristics of brake pads [26]. To evaluate the temperature increase under varied speeds and constant braking force, a brake test was employed for all composite materials of the brake pad. All samples get an equal application of braking force. The test involves braking circumstances speeds between 200 and 500 rpm. An infrared thermometer is used to measure the rise in temperature of the brake pad surface.

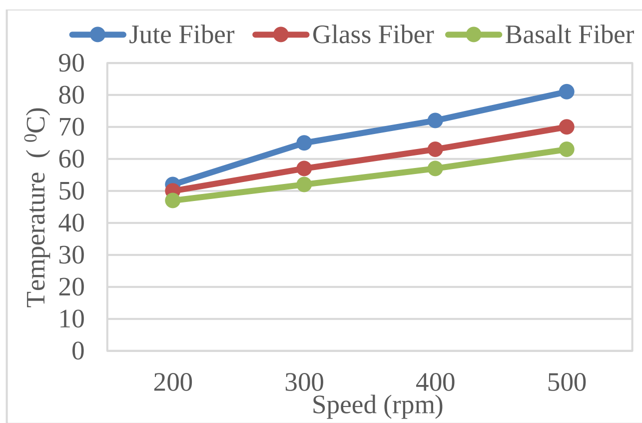

Fig. 5 Speed vs. Temperature Rise of Brake Pad

Figure 5 illustrates that the basalt fiber pad has better heat resistance and conductivity than glass and jute fiber; it has the lowest temperature rise, about 20-30% less than glass fiber and 40–50% less than jute fiber. The temperature rise of glass fiber brake pads was moderate; it was around 15-25% lower than that of basalt but 20-30% greater than that of jute. Jute fiber brake pads are less effective for high-braking performance due to the biggest temperature rise, usually 40-50% more than basalt and 15-25% higher than basalt glass pads.

5.3. Cooling Effect Test of Composite Brake Pad

The cooling effect test of brake pads evaluates how efficiently brake pads dissipate heat after braking. Used to measure the temperature drop over time. The test is conducted under identical conditions for all materials. Simulating braking conditions measure the temperature variations and monitor the temperature decrease over time. The braking system setup consists of a rotating free disc for different speeds while a data logger captures changes in real-time temperature readings. The cooling effect of the specified composite brake pad is depicted in Figure 6.

As time increases, the cooling rate of each brake pad also rises, following the typical environmental conditions [27-28]. However, due to its inherent properties, the cooling effect is determined based on its selected working conditions. Figure 6 indicates basalt fiber brake pads are the best choice for efficient heat dissipation and cooling, making them ideal for high-performance or heavy-duty braking systems. Basalt fiber brake pads offer a good compromise between cooling efficiency and environmental friendliness, performing well under moderate braking conditions. Basalt fibre brake pads have the highest cooling efficiency, 42.5%, whereas the cooling efficiency of the glass fibre brake pad was 35.71%, and that of the jute fibre brake pad was 27.77%, respectively. The cooling efficiency of the basalt brake pad is 18% better than that of a jute and 7-8% better than that of a glass fibre brake pad.

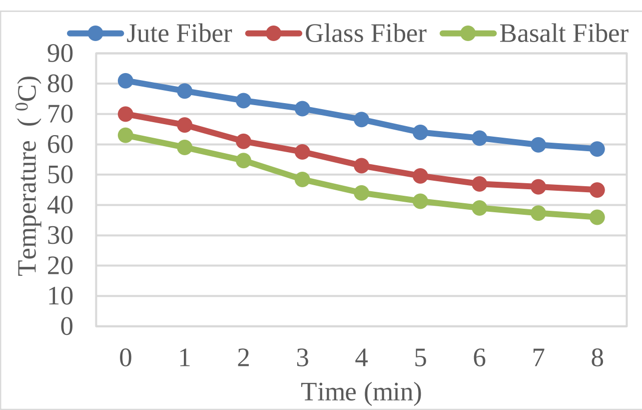

Fig. 6 Cooling Effect of Composite Brake Pad

6. Conclusion

Designed test rig successfully validated for the braking performance of composite materials of brake pads. The test rig successfully simulated real-world braking scenarios, enabling a comprehensive assessment of stopping time, cooling efficiency, and heat rise of each material. The following conclusions are drawn from the performance test results of brake pads.

A designed brake test rig satisfactorily worked to measure the temperature rise, cooling rate, and deceleration performance of the brake pad under various conditions. The test rig provided accurate, consistent, and repeatable measurements, ensuring reliable comparisons between different materials.

- Basalt fibre brake pads demonstrated the best overall performance, with a cooling efficiency of 42.5%, the shortest stopping time (24 sec), and excellent heat resistance, making them ideal for high-performance braking applications.
- Glass fibre brake pads showed moderate performance, with 35.71% cooling efficiency and 24-sec stopping time, making them suitable for medium-duty applications.
- Jute fibre brake pads had the lowest efficiency (27.77%), with the longest stopping time (30 sec) and higher heat retention, making them less suitable for high-speed braking but feasible for light-duty applications.

Finally, the experimental results showed that the developed brake pad test rig offered a highly reliable and precise assessment of the cooling efficiency, temperature rise, and stooping time of composite brake pads. The findings of this study show that basalt fiber can possibly be used in place of asbestos brake pad materials.

Nomenclature

ΔR	Weight transferred on the front axle	μ_p	Poisons ratio of flywheel material
l	Wheel base of vehicle	v	Peripheral velocity
g	Gravitational force	M_t	Torsional moment
h	Height of C.G from ground	R_s	Radius of shaft
M	Total mass of vehicle	J	Polar moment of inertia of shaft
μ	Coefficient of friction bet. tire & road	τ	Torsional shear stress
R_{fs}	Static weight of front axle	K_b	Shock factor
w_f	Weight of front axle	K_t	Fatigue factor
m_f	Mass of front axle	M_b	Bending moment
F	Friction Force	m_g	Module of gear
T_B	Torque at the wheel	kW	Power transmitted by gears
R	Radius of wheel	C_S	Service factor
m	Mass of the flywheel	fs	Factor of safety
r	Radius of flywheel	z_p	Number of teeth on the pinion
V	Maximum velocity	n_p	Speed of pinion
I	Mass moment of inertia of the flywheel	C_V	Velocity Factor

ω	Angular velocity of flywheel	b	Face width of gear tooth
ρ	Mass density of flywheel material	S_{ut}	Ultimate tensile strength

σ_t	Tangential stress at the flywheel	Y	Lewis form factor
σ_r	Radial stress at flywheel	KE	Kinetic energy

References

[1] S. Vigneshwarans et al., "Recent Advancement in the Natural Fiber Polymer Composites: A Comprehensive Review," *Journal of Cleaner Production*, vol. 277, 2020. [CrossRef] [Google Scholar] [Publisher Link]

[2] S. Sri Karthikeyan et al., "Elemental Analysis of Brake Pad Using Natural Fibres," *Materials Today: Proceedings*, vol. 16, pp. 1067-1074, 2019. [CrossRef] [Google Scholar] [Publisher Link]

[3] Mithul Naidu et al., "An Insight on the Influence of Fiber Content on Plant Fiber Reinforced Brake Pads," *International Journal of Future Generation Communication and Networking*, vol. 13, no. 2s, pp. 1070-1082, 2020. [Google Scholar]

[4] J. Jefferson Andrew, and H.N. Dhakal, "Sustainable Biobased Composites for Advanced Applications: Recent Trends and Future Opportunities – A Critical Review," *Composites Part C: Open Access*, vol. 7, pp. 1-32, 2022. [CrossRef] [Google Scholar] [Publisher Link]

[5] Tej Singh, "Optimum Design based on Fabricated Natural Fiber Reinforced Automotive Brake Friction Composites using Hybrid CRITIC-MEW Approach," *Journal of Materials Research and Technology*, vol. 14, pp. 81-92, 2021. [CrossRef] [Google Scholar] [Publisher Link]

[6] Naresh Kumar et al., "Experimental Investigation on the Physical, Mechanical and Tribological Properties of Hemp Fiber-based Non-Asbestos Organic Brake Friction Composites," *Materials Research Express*, vol. 6, no. 8, 2019. [CrossRef] [Google Scholar] [Publisher Link]

[7] C. Pinca-Bretotean et al., "Friction and Wear Characteristic of Organic Brake Pads Material," *IOP Conference Series: Materials Science and Engineering: International Conference on Applied Sciences*, Banja Luke, Bosnia and Herzegovina, vol. 477, pp. 1-8, 2019. [CrossRef] [Google Scholar] [Publisher Link]

[8] A. Jacob Moses, A. Suresh Babu, and S. Ananda Kumar, "Analysis of Physical Properties and Wear Behavior of Phenol Formaldehyde – Basalt Fiber Reinforced Brake Pad," *Materials Today: Proceedings*, vol. 33, pp. 1128-1132, 2020. [CrossRef] [Google Scholar] [Publisher Link]

[9] Dipen Kumar Rajak et al., "Recent Progress of Reinforcement Materials: A Comprehensive Overview of Composite Materials," *Journal of Materials Research & Technology*, vol. 8, no. 6, pp. 6354-6374, 2019. [CrossRef] [Google Scholar] [Publisher Link]

[10] Mithul Naidu et al., "Wear and Friction Analysis of Brake Pad Material Using Natural Hemp Fibers," *Polymers*, vol. 15, no. 1, pp. 1-11, 2022. [CrossRef] [Google Scholar] [Publisher Link]

[11] İbrahim Mutlu, İlker Sugözü, and Ahmet Keskin, "The Effects of Porosity in Friction Performance of Brake Pad using Waste Tire Dust," *Polímeros*, vol. 25, no. 5, pp. 440-446, 2015. [CrossRef] [Google Scholar] [Publisher Link]

[12] Taiwo Oseni Oladokun et al., "Effect of Moulding Pressure on Brake Lining Produced from Industrial Waste Material: Sawdust," *European Journal of Engineering Research and Science*, vol. 4, no. 6, pp. 62-68, 2019. [CrossRef] [Google Scholar] [Publisher Link]

[13] Amirhossein Hatam, and Abolfazl Khalkhali, "Simulation and Sensitivity Analysis of Wear on the Automotive Brake Pad," *Simulation Modelling Practice and Theory*, vol. 84, pp. 106-123, 2018. [CrossRef] [Google Scholar] [Publisher Link]

[14] Hasan Öktem, Ilyas Uygur, and Murat Çevik, "Design, Construction and Performance of a Novel Brake Pad Friction Tester," *Measurement*, vol. 115, pp. 299-305, 2018. [CrossRef] [Google Scholar] [Publisher Link]

[15] Luca Vecchiato et al., "Design and Development of a Brake Test Bench for Formula SAE Race Cars," *Machines*, vol. 12, no. 2, pp. 1-17, 2024. [CrossRef] [Google Scholar] [Publisher Link]

[16] Chang-Hee Yoo, Jin-Hwan Park, and Sang-Shin Park, "Design and Evaluation of Performance Tester for Yaw Brakes in Wind Turbines," *International Journal of Precision Engineering and Manufacturing-Green Technology*, vol. 5, pp. 81-87, 2018. [CrossRef] [Google Scholar] [Publisher Link]

[17] Bhau Kashinath Kumbhar, Satyajit Ramchandra Patil, and Suresh Maruti Sawant, "A Comparative Study on Automotive Brake Testing Standards," *Journal of The Institution of Engineers (India): Series C*, vol. 98, pp. 527-531, 2017. [CrossRef] [Google Scholar] [Publisher Link]

[18] Zeng-Cheng Liao et al., "Design, Modeling, and Verification of a Test Bench for Braking Simulation of 1/4 Vehicle," *Proceedings of the Institution of Mechanical Engineers, Part D: Journal of Automobile Engineering*, vol. 234, no. 5, pp. 1425-1441, 2019. [CrossRef] [Google Scholar] [Publisher Link]

[19] Mustafa Timur, Hilmi Kuşçu, and Hayrettin Toylan, "Design and Manufacture of Automated Controlled test Machine Detecting Braking Characteristic of Brake Lining in Vehicles," *Proceedings of the Institution of Mechanical Engineers, Part C: Journal of Mechanical Engineering Science*, vol. 231, no. 18, pp. 3318-3329, 2016. [CrossRef] [Google Scholar] [Publisher Link]

[20] Marzieh Salehi et al., "Parameter Optimization for a Laboratory Friction Tester to Predict tire ABS Braking Distance using Design of Experiments," *Materials and Design*, vol. 194, pp. 1-13, 2020. [CrossRef] [Google Scholar] [Publisher Link]

[21] K.W. Liew, and Umar Nirmal, "Frictional Performance Evaluation of Newly Designed Brake Pad Materials," *Materials and Design*, vol. 48, pp. 25-33, 2013. [CrossRef] [Google Scholar] [Publisher Link]

[22] Lü Hui, and Yu Dejie, "Optimization Design of a Disc brake System with Hybrid Uncertainties," *Advances in Engineering Software*, vol. 98, pp. 112-122, 2016. [CrossRef] [Google Scholar] [Publisher Link]

[23] Sayed Nashit et al., "Design, Fabrication and Testing of Regenerative Braking Test Rig for BLDC Motor," *International Research Journal of Engineering and Technology*, vol. 3, no. 5, pp. 1881-1884, 2016. [Google Scholar] [Publisher Link]

[24] P. Saravanan, Y. Agatheesh Senthil, and M. Prethish Haran, "A Complete Study on Natural Fibre Reinforced Composites Used in Brake Pads," *International Journal of Science, Engineering and Technology*, vol. 10, no. 1, pp. 1-8, 2022. [Publisher Link]

[25] R.J. Talib et al., "Aptness of Kenaf Powder as a Friction Modifier in the Fabrication of Brake Friction Material by Powder Metallurgy Route," *Jurnal Tribologi*, vol. 19, pp. 121-131, 2018. [Google Scholar] [Publisher Link]

[26] S. Senthil Kumaran, "Study of Raw and Chemically Treated Sansevieria Ehrenbergii Fibers for Brake Pad Application," *Materials Research Express*, vol. 7, no. 5, pp. 1-17, 2020. [CrossRef] [Google Scholar] [Publisher Link]

[27] Weitao Sun, and Wenlong Zhou, "Effects of Friction Film Mechanical Properties on the Tribological Performance of Ceramic Enhanced Resin Matrix Friction Materials," *Journal of Materials Research and Technology*, vol. 8, no. 5, pp. 4705-4712, 2019. [CrossRef] [Google Scholar] [Publisher Link]

[28] Gai Peter Friday et al, "Physico-Mechanical Properties of Basalt-based Brake Pad as Alternative to Ceramics Brake Pad," *Saudi Journal of Engineering and Technology*, vol. 7, no. 1, pp. 16-33, 2022. [Google Scholar] [Publisher Link]